Nonlinear index of a two-level model: The essential role of the population inversion

Hervé Leblond and Charles Ciret

Laboratoire de Photonique d'Angers, EA 4464, Université d'Angers, 2 Boulevard Lavoisier, 49000 Angers, France

Optical wave propagation in an assembly of two-level atoms is considered. An asymptotic model of nonlinear Schrödinger (NLS) type is derived in a rigorous way by means of the perturbative expansion method. The results of the obtained model are then compared with both a numerical solution of the initial set of equations of the two-level model and an exact analytical cnoidal wave solution. It is seen that the evolution of the population difference is a key factor for the accurate determination of the nonlinear index, and that the NLS approximation allows one to determine it theoretically. The knowledge of the population difference allows one to correct the cnoidal wave solution, which then matches the numerical solution up to the limits of our numerical accuracy.

I. INTRODUCTION

Key parameters of nonlinear optics are the nonlinear coefficients, among which the nonlinear index commonly denoted by n_2, which measures the strength of the Kerr effect and self-focusing, has a prominent place. This quantity can be measured by several methods, among which the most known is probably the z-scan technique [1].

Other methods are used, and the z-scan itself has been improved (see, e.g., [2,3]), yielding a considerable improvement of the accuracy of the nonlinear index measurements. Accurate measurements show in turn that as it could be expected from theoretical speculation, the evolution of the refractive index with respect to the incident optical intensity ceases to be linear for high enough input intensity. A first correction to the nonlinear index, the so-called fifth-order nonlinear refractive index n_4, has been measured [4–8].

The theoretical description of the nonlinear changes in the refractive index, however, remains, in large part, phenomenological. It rests mainly on the theory of nonlinear susceptibilities, first introduced from a quantum mechanical approach [9,10], but which can also be obtained from a classical model [11]. The susceptibility approach is almost always restricted to the leading order. Its generalization to higher orders, indeed, although possible in principle, involves excessively complicated computations and such attempts are quite rare [12]. The susceptibility approach belongs to the family of perturbations approaches, and such a catastrophic increase of complexity when considering higher-order terms is very generally an intrinsic defect of them. In this paper, however, we restrict ourselves to a two-level medium, and an exact periodic solution of the wave equation has been found in this case [13]. It overcomes the intrinsic difficulties due to perturbations, at least within this restricted frame, up to huge values of the optical intensity. Both the exact solution and the susceptibility theory have been compared to the exact numerical solution of the two-level model equations, which has the advantage, with respect to an experiment, of being insensitive to any doubtful issue about the modeling itself. The analysis made it clear that the susceptibility approach needs to be improved, even at moderate input intensities [14].

Its major defect, besides the intrinsic limitations of any perturbation scheme, is that it computes a response of the material to the wave without taking into account the feedback of the material on the wave. This requires one to consider the evolution of both the wave field and the material characteristics; the perturbation approach that does this is known as the perturbative expansion method [15,16]. It is usually used to derive simplified asymptotic model equations for the wave field. The relevant asymptotic model for the description of the optical Kerr effect and of the self-focusing is the nonlinear Schrödinger (NLS) equation. It was first introduced in [17] and completely solved in [18].

It is well known that in a medium presenting a quadratic nonlinearity, far enough from phase matching, an effective Kerr effect arises due to the so-called cascading effect: a second harmonic is generated and interacts quadratically with the fundamental incident wave [19,20]. Theoretical computations show that another process should have a comparable importance, this process is the formation of a wave with a typical period comparable to the pulse length by optical rectification, which in turn modifies the index through the electro-optic effect. If spatiotemporal behavior is considered, this process leads to an asymptotic model which is not merely the NLS equation, but contains an additional field variable describing the slow wave, known as the Davey-Stewartson system [21,22]. The rigorous mathematical proof of the validity of the perturbative expansion method that leads to NLS has shown that this process cannot, in principle, be neglected [23]. This remains obviously true when the quantity which results from the quadratic nonlinearity is not observable directly, but only by its effects on others. We will see that it happens with the population difference in a two-level medium.

II. MODEL AND KNOWN RESULTS

We consider a linearly polarized electromagnetic plane wave propagating in an assembly of identical two-level atoms.

The fundamental and excited states are labeled 1 and 2 and have energies $\hbar\omega_a$ and $\hbar\omega_b$, respectively, so that the transition frequency is $\Omega = \omega_b - \omega_a > 0$. The Schrödinger–von Neumann and the wave equations can be reduced to the system [13]

$$\frac{\partial \mathcal{W}}{\partial t} = \frac{-2}{\hbar} qE, \tag{1}$$

$$\frac{\partial d}{\partial t} = -\Omega q, \tag{2}$$

$$\frac{\partial q}{\partial t} = \Omega d + 2\frac{|\mu|^2}{\hbar}\mathcal{W}E, \tag{3}$$

$$\frac{\partial E}{\partial t} = -c^2\frac{\partial B}{\partial z} + \frac{N}{\varepsilon_0}\Omega q, \tag{4}$$

$$\frac{\partial B}{\partial t} = -\frac{\partial E}{\partial z}. \tag{5}$$

Here, t and z are the time and space variables, and E and B are the wave electric field and magnetic induction. The population difference is defined as

$$\mathcal{W} = \rho_{22} - \rho_{11}, \tag{6}$$

where ρ is the density matrix operator. Also,

$$d = \rho_{12}\mu^* + \rho_{21}\mu, \tag{7}$$

where μ is the atomic electric dipole transition moment, is the atomic dipole momentum, and the quantity

$$q = -i(\rho_{12}\mu^* - \rho_{21}\mu) \tag{8}$$

contains all remaining components of the density matrix. c is the speed of light in vacuum, ε_0 the dielectric permittivity in vacuum, and N the density of atoms.

An exact cnoidal wave solution to Eqs. (1)–(5) was derived in [13], and reads as

$$E = E_m cn\left(p\left[t - \frac{z}{v}\right], k\right), \tag{9}$$

$$B = \frac{E}{v}, \tag{10}$$

$$\mathcal{W} = \frac{\varepsilon_0}{N\hbar}\frac{\chi}{\Omega}E^2 - l, \tag{11}$$

$$d = \frac{\varepsilon_0}{N}\chi E, \tag{12}$$

and

$$q = \frac{\varepsilon_0\hbar}{N|\mu|}\frac{\chi k p^2}{\Omega}sn\left(p\left[t - \frac{z}{v}\right]\right)dn\left(p\left[t - \frac{z}{v}\right]\right), \tag{13}$$

where cn, sn, and dn are Jacobi's elliptic functions,

$$\chi = \frac{c^2}{v^2} - 1 = \frac{2lN|\mu|^2\Omega}{\varepsilon_0\hbar[\Omega^2 - p^2(1 - 2k^2)]}, \tag{14}$$

and

$$E_m = \frac{\hbar}{|\mu|}kp. \tag{15}$$

Here, l is the value of $-\mathcal{W}$ at infinity, assumed to be its value at thermal equilibrium. These formulas yield a two-parameter family of solutions, determined by the elliptic modulus

k ($0 \leqslant k \leqslant 1$), and parameter p which relates to the wave angular frequency ω through

$$\omega = \frac{\pi p}{2K(k)}, \tag{16}$$

where $K(k)$ is the elliptic integral of the first kind.

III. DERIVATION OF THE NLS APPROXIMATION FOR THE TWO-LEVEL MODEL

A. Assumptions and expansions

A NLS equation was derived from a slightly more general model in [25]. As the susceptibility theory does, it neglects the mean value or zero-order harmonic of the population difference $\mathcal{W}$. A more rigorous derivation, taking this term into account, is outlined below, the details of which can be found in the Appendix. It follows the reductive perturbation method [15,16,23]. Recall that this asymptotic method mainly consists in accounting for the cumulative effects of small corrections over long propagation distances, through an approximate equation satisfied by the leading term in the expansion.

A small parameter ε is introduced, which measures both the narrowness of the spectral width (slowly varying envelope approximation) and the relative smallness of the amplitude with respect to the atomic field (small amplitude assumption). Slow variables are defined as

$$\tau = \varepsilon\left(t - \frac{z}{V}\right) \quad \text{and} \quad \zeta = \epsilon^2 z, \tag{17}$$

where V will be shown to be the group velocity. The electric field, and other dependant variables $\mathcal{W}$, q, and d, are expanded in both a Fourier series of the fundamental phase $\varphi = (\kappa z - \omega t)$ and in a power series of ε [see Eq. (A2) in the Appendix]. It is assumed that, at leading order, the electric field is

$$E = \varepsilon\mathcal{E}e^{i\varphi} + cc + O(\varepsilon^3); \tag{18}$$

further assumptions are detailed in the Appendix. $\mathcal{E} = E_1^{(1)}(\tau, \zeta)$ is the envelope of the wave field, modulating a fast oscillating wave with phase φ. It will be shown that $\mathcal{E}$ obeys the NLS equation.

B. Resolution of the perturbation scheme

The perturbation scheme is then solved order by order. At first order is found, as usual, the dispersion relation, which we express by the linear refractive index n_0 given by

$$n_0^2 = 1 + \frac{2Nl|\mu|^2}{\varepsilon_0\hbar}\frac{\Omega}{\Omega^2 - \omega^2}. \tag{19}$$

We also obtain proportionality relations between the first-order components of E, $\mathcal{W}$, d, and q, which determine a linear propagation mode with well-defined velocity $v_L = c/n_0$.

At second order, it is found that all second-harmonic terms are zero, except $\mathcal{W}_2^{(2)}$ which is proportional to $\mathcal{E}^2$ [see Eq. (A6)]. The fundamental frequency terms satisfy $\mathcal{W}_2^{(1)} = 0$; at the same order is found, as usual, that V is the group velocity, $V = v_g$.

At order ε^3, third-harmonic terms are obtained for d, q, and $\mathcal{E}$, which are not needed to obtain the asymptotic equation,

but will be used in the approximate solution which will be compared to numerical results. The expressions of these terms present, in the denominator, a factor $\Omega^2 - 9\omega^2$, which seems to express a resonance as the third-harmonic frequency of the wave coincides with the transition frequency. We will see that this resonance factor vanishes in the final asymptotic expression of the solution. In contrast, the population difference $\mathcal{W}$ does not contain a third-harmonic term.

At third order, we show that $\mathcal{E}$ satisfies a differential equation of the form

$$i\frac{\partial \mathcal{E}}{\partial \zeta} + \mathcal{A}\frac{\partial^2 \mathcal{E}}{\partial \tau^2} + \mathcal{B}\mathcal{E}|\mathcal{E}|^2 + \mathcal{C}\mathcal{W}_2^{(0)}\mathcal{E} = 0, \qquad (20)$$

where

$$\mathcal{B} = \frac{-2Nl|\mu|^4}{\varepsilon_0\hbar^3 cn_0}\frac{\Omega\omega}{(\Omega^2 - \omega^2)^2}, \qquad (21)$$

and $\mathcal{C}$ is given by Eq. (A15) (see the Appendix). Computation shows that $\mathcal{A} = -\kappa_2/2$, where

$$\kappa_2 = \frac{d^2\kappa}{d\omega^2} \qquad (22)$$

is the group velocity dispersion.

C. Zero-order harmonic

The key element of the present paper is the shift of the zero-order harmonic, or mean value, of the population difference with respect to its thermal value $\mathcal{W}_0^{(0)} = -l$. Its leading term is $\mathcal{W}_2^{(0)}$; if it is ignored, as does the susceptibility theory and as it was done in [25], Eq. (20) straightforwardly reduces to the NLS equation, and the nonlinear coefficient $\mathcal{B}$ coincides with the coefficient derived from the susceptibility theory (see [14]).

However, the general theory of the perturbative expansion method (see [16,23]) shows that great care must be taken of the zero-harmonic component.

The relevant component of $\mathcal{W}$, $\mathcal{W}_2^{(0)}$ is found at third order, from the integration of a differential equation [see Eq. (A16)]; it is proportional to $|\mathcal{E}|^2$.

Inserting the obtained expression into Eq. (20) yields

$$i\frac{\partial \mathcal{E}}{\partial \zeta} - \frac{\kappa_2}{2}\frac{\partial^2 \mathcal{E}}{\partial \tau^2} + \Gamma\mathcal{E}|\mathcal{E}|^2 = 0, \qquad (23)$$

which is known as the NLS equation [18], with

$$\Gamma = \frac{-Nl|\mu|^4\omega\Omega(3\Omega^2 + \omega^2)}{n_0\epsilon_0 c\hbar^3(\Omega^2 - \omega^2)^3}. \qquad (24)$$

Note that this value may also be found in [24] [Eq. (3.26)], but without proof.

D. Solution of constant amplitude of NLS and Kerr effect

The NLS equation (23) admits the constant amplitude solution

$$\mathcal{E} = \mathcal{A}e^{i\Gamma\mathcal{A}^2\zeta} \qquad (25)$$

(a more general form including a frequency shift exists, but it is not useful here). Using (18) and the definition of the slow

variables (17), we put expression (25) in the form

$$E \simeq E_m \cos\left[\omega\left(t - \frac{z}{v}\right)\right], \qquad (26)$$

with $E_m = 2\varepsilon\mathcal{A}$ and

$$\frac{\omega}{v} = \kappa + \frac{\Gamma}{4}E_m^2. \qquad (27)$$

The wave defined by (25) appears to be an approximate periodic solution, with constant amplitude and angular frequency ω of the two-level model. Consequently, one would expect that it would coincide with the exact cnoidal wave solution with same angular frequency and same small amplitude, which is Eq. (9) at the limit where k tends to zero.

To investigate this hypothesis, the complete approximate solution is required. In the course of the derivation, it is found that the population difference $\mathcal{W}$ contains both a second-harmonic term and a rectified one, which have been determined [see the Appendix, esp. Eqs. (A19), (A6), and (A16)]. Explicit computation yields

$$\mathcal{W}_{\text{NLS}} = -l + \frac{l|\mu|^2(\Omega^2 + \omega^2)E_m^2}{\hbar^2(\Omega^2 - \omega^2)^2}$$
$$+ \frac{l|\mu|^2 E_m^2}{\hbar^2(\Omega^2 - \omega^2)}\cos 2(\kappa_{\text{NLS}}z - \omega t). \qquad (28)$$

The atomic dipole can be computed in an analogous way, and we eventually obtain the expression

$$d_{\text{NLS}} = \left[\frac{\varepsilon_0}{N}\chi^{(1)}(\omega)E_m + a_1 E_m^3\right]\cos(\kappa_{\text{NLS}}z - \omega t)$$
$$+ a_3 E_m^3\cos 3(\kappa_{\text{NLS}}z - \omega t). \qquad (29)$$

The explicit expression of coefficients a_1 and a_3 is given by Eqs. (A21) and (A22) in the Appendix. It should be noticed that the factor $(\Omega^2 - 9\omega^2)$, which accounts for a resonance as 3ω approaches the transition frequency Ω, which appeared in some terms involved in the computation of d, completely vanishes from its final expression due to algebraic simplification.

We shown in [14] that the third-harmonic resonance predicted by the nonlinear susceptibility formalism was not seen in the numerical solution or in the cnoidal wave one. In the same way, no third-harmonic resonance is predicted by the NLS approach.

From an analogous procedure, we get the approximate solution for q as

$$q_{\text{NLS}} = \frac{-\omega}{\Omega}\left[\frac{\varepsilon_0}{N}\chi^{(1)}(\omega)E_m + a_1 E_m^3\right]\cos(\kappa_{\text{NLS}}z - \omega t)$$
$$- \frac{3\omega}{\Omega}a_3 E_m^3\cos 3(\kappa_{\text{NLS}}z - \omega t), \qquad (30)$$

using same the coefficients a_1 and a_3 as above.

IV. COMPARISON BETWEEN NLS AND NUMERICS

A. NLS works well for moderate intensities.

The system (1)–(5) is solved numerically by means of a standard fourth-order Runge-Kutta scheme with respect to time t, with the z derivatives being computed by fifth-order

finite-difference formulas. We use periodic boundary conditions, especially to avoid instabilities on the boundaries. This scheme allows one to solve the evolution with respect to time t of an initial state given for all z at some fixed time.

In order to model the response of the medium to a monochromatic input, we use the same procedure as in [14]. The computation box is divided into two parts, the first of which represents vacuum and the second the medium, and the initial condition is chosen to be some square pulse localized in the vacuum and propagating towards the medium.

In the medium, i.e., for $0 < z < L$, where $2L$ is the size of the computation box, the transition dipole moment μ takes some nonzero value, while the vacuum is modeled by setting μ to zero for $-L < z < 0$. To reduce reflections and improve numerical stability, instead of a square pulse, we use as an input a super-Gaussian profile, as

$$E(t=0) = \omega_w k \cos\left(\frac{\omega_w z}{c}\right) \exp\left[-\left(\frac{z-z_c}{\Delta z}\right)^s\right], \quad (31)$$

with $B(t=0) = E(t=0)/c$, $d(t=0) \equiv 0$, $\mathcal{W}(t=0) \equiv -l$, and $q(t=0) \equiv 0$. We found it convenient to use a high super-Gaussian order $s = 20$, and parameters $z_c = -L/2$, $\Delta z = 0.45L$.

This approach quite closely models the physical response of a medium to an input beam, insofar that the medium can be described by a two-level model.

Reflections occur at the interfaces $z = 0$ and $z = \pm L$, and the study is thus limited to a space-time domain where the backward reflected waves do not perturb the forward transmitted ones.

The expression (19) of the linear index n_0 shows that propagation is impossible for

$$\Omega < \omega < \omega_1 = \sqrt{\Omega^2 + \frac{2Nl|\mu|^2\Omega}{\varepsilon_0\hbar}}. \quad (32)$$

From (24), it is seen that the nonlinear coefficient Γ of the NLS equation changes its sign at $\omega = \Omega$, it is positive for frequencies above the resonance ($\omega > \omega_1$), and negative below it ($\omega < \Omega$). Elementary analysis shows that κ_2 is positive for ω below some angular frequency ω_0, which lies in the domain where no propagation occurs ($\Omega < \omega_0 < \omega_1$). As a result, $\kappa_2 > 0$ for $\omega < \Omega$ and negative for $\omega > \omega_1$, and the product $-\kappa/2 \times \Gamma$ is always positive. Hence the NLS equation (23) always supports solitons, and its constant amplitude solution is unstable through modulation instability [26,27]. Notice that if the population difference $\mathcal{W}_0$ is disregarded, the nonlinear coefficient Γ in the NLS equation is replaced with the coefficient $\mathcal{B}$ of Eq. (20), given by (21). It is seen that $\mathcal{B}$ is always negative, and hence this erroneous value of the nonlinear coefficient would predict a defocusing NLS, without soliton formation, for frequencies above the resonance. Numerical resolution of system (1)–(5) shows that modulation instability and soliton formation actually occur.

The analysis must be restricted to the time-space domain were the instability did not yet develop, and the continuous wave still exists. This is consequent with nonlinear index measurements, which also must be performed before soliton formation occurs, although spatial transverse instability is more frequently involved in experiments than longitudinal temporal one.

For technical reasons, among others, in order to reduce spurious reflections, the refraction index must not be far from one. Therefore, we use a quite low transition dipole moment, set to $\mu = 0.3ea_0$, where $a_0 = 4\pi\varepsilon_0\hbar^2/(me^2)$ is the Bohr radius (with m and $-e$ the mass and electric charge of the electron). For numerical convenience, we inspect the behaviors below and above resonance with two different values of the resonance wavelength, namely, $\lambda_r = 0.5\ \mu$m and $1.7\ \mu$m. The length of the computation box is close to $120\ \mu$m, half of which represents the medium, and the evolution time is 500 fs or 600 fs. However, the domain where the wave can be considered as having constant amplitude is much smaller.

The velocity of the numerical solution is evaluated with the same method as detailed in [14]: each of the relations $v = E/B$ and $\chi = d/E$ allows the computation of an approximation of the velocity v, the effective susceptibility χ, and the effective index $n = c/v = \sqrt{1+\chi}$, provided that the ratio of the two fields can be estimated. This cannot be achieved in direct space because of huge inaccuracies when the denominators vanish, but can be in Fourier space. We check that the difference between the two estimates is always much smaller than the accuracy of the analytical expressions under investigation.

The cnoidal wave model is computed through Eqs. (9)–(13), with the velocity given by (14); the parameters p and k are found by numerically solving Eqs. (16) and (15), for fixed values of the angular frequency ω and the maximal amplitude E_m. ω is set to its input value, which is well conserved by the computation, and E_m is evaluated from the numerical data, by taking the maximum of $|E|$ over a domain where the wave amplitude can be considered as constant, which seems to be the most accurate way to do it.

The NLS approximation is given by (26) and (28)–(30), with the same amplitude and angular frequency as above and the velocity (27).

Let us first consider frequencies below the resonance ($\omega < \Omega$). We use $\lambda_r = 0.5\ \mu$m, which yields $\Omega = 3.7699$ rad fs^{-1}, angular frequencies ranging from 2 to 3 rad fs^{-1}, and values of the elliptic modulus k ranging from 0.15 to 0.8, which would correspond to input intensities ranging from 7600 GW/cm^2 to a huge value as $370 \times$ TW/cm^2. A strong enough nonlinearity is required, on one hand, in order to decrease the computation time and box size, and, on the other hand, in order to increase the nonlinear shift of the index well above the limited numerical accuracy. Huge intensities are considered to investigate the domain where the NLS approximation will fail.

All components E, w, d, and q of the numerical solution can be compared to the corresponding analytic expressions, as given by both the cnoidal wave solution and the NLS approximation; see an example in Fig. 1. The agreement is quite satisfactory, and it has been shown in [14] that it is much better than the theory of susceptibilities. Notice, however, that appreciable fluctuations of $\mathcal{W}$, d, and q, i.e., all components of the density matrix, occur immediately after the interface ($z = 0$). Some shift of the population difference $\mathcal{W}$ can be
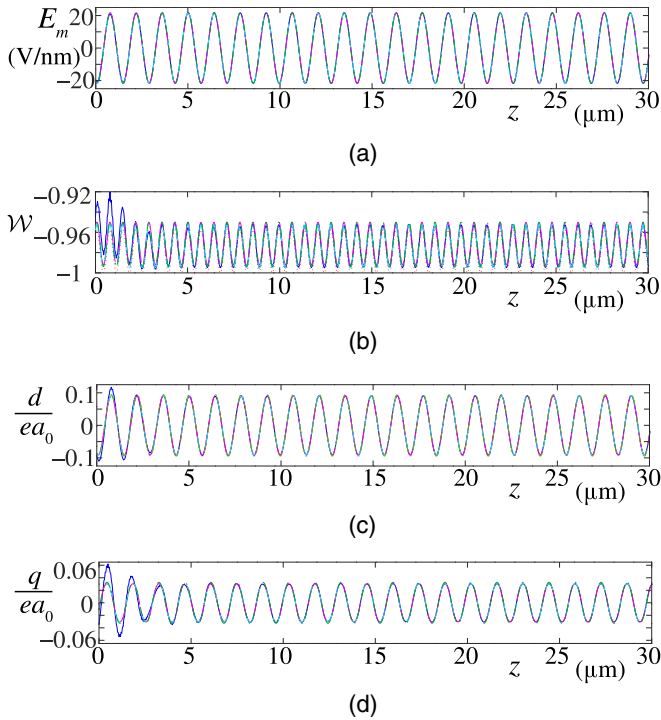
FIG. 1. The evolution of a square pulse, (a) electric field E, (b) population difference $\mathcal{W}$, (c) atomic dipole momentum d, (d) auxiliary field q. For clarity, only a small part of the computation box (one-eighth) is shown, starting just at the interface. Blue solid line: numerical solution; red dotted line: cnoidal wave solution; green dash-dotted line: NLS approximation; pink long dashes: cnoidal wave solution corrected according to $\mathcal{W}_0$ given by the NLS approximation; light-blue short dashes: cnoidal wave solution corrected according to the numerically obtained value of $\mathcal{W}_0$. The resonance wavelength is $\lambda_r = 0.5$ µm, and the parameters of the initial data are $\omega_w = 1.3092$ rad fs^{-1}, $k = 0.4$.

seen; it is reproduced by the NLS model, not by the cnoidal wave solution.

Since only a few optical oscillations are represented in Fig. 1, the difference in the velocities obtained for the various solutions can hardly be seen. Figure 2 shows a set of values of the nonlinear shift Δn_{NL} of the refraction index for a moderate nonlinearity determined by the elliptic modulus $k = 0.15$, which would correspond, for the choice of the other parameters, to input intensities ranging between about 7600 to about 8800 GW/cm^2. It is seen that the NLS approximation (green line) yields a much better approximation of the numerical solution (blue line) than the cnoidal wave solution (red line) (the two remaining curves will be discussed later). It remains true for a a much stronger nonlinearity; however, the improvement is less important. See in Fig. 3 the example of $k = 0.4$, which would correspond to intensities about 61 to 63 TW/cm^2, for analogous parameters. Here the error resulting from the use of the cnoidal solution is twice the error arising with NLS (with opposite sign), while the same factor is about 5 for the case of a weaker nonlinearity, shown in Fig. 2.

An example of the evolution of the various estimations of Δn_{NL} as a function of the wave amplitude E_m is shown in Fig. 4. Here, E_m is the actual amplitude in the medium, as
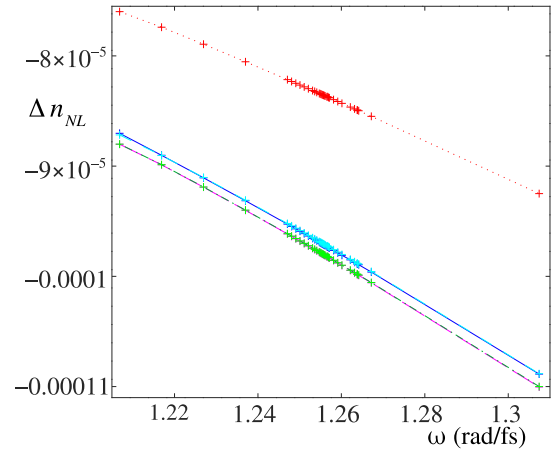

FIG. 2. The nonlinear shift of the refractive index Δn_{NL} vs the wave angular frequency ω_w, for an elliptic modulus $k = 0.15$. The color code is the same as in Fig. 1. The resonance wavelength is $\lambda_r = 0.5$ µm.
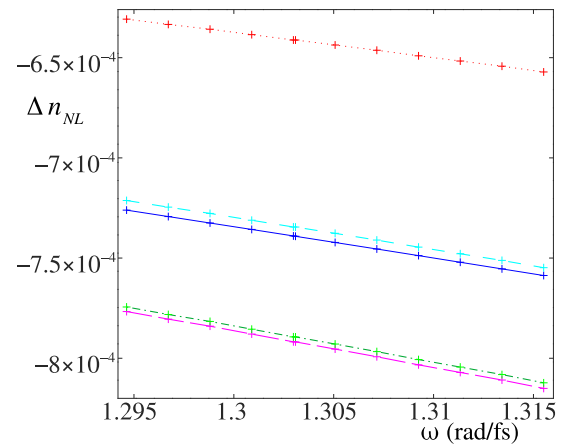

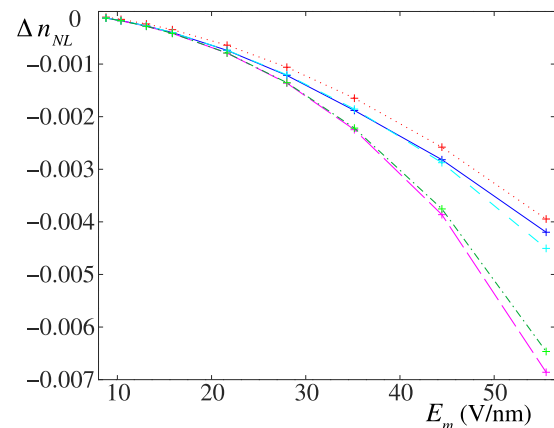FIG. 3. Same as Fig. 2, but with elliptic modulus $k = 0.4$.

FIG. 4. The nonlinear shift Δn_{NL} of the refractive index against the wave amplitude E_m. The color code is the same as in Fig. 1. The input assumes $p = 1.2481$ rad fs^{-1}, with an elliptic modulus k varying from 0.17 to 0.8. The resonance wavelength is $\lambda_r = 0.5$ µm.
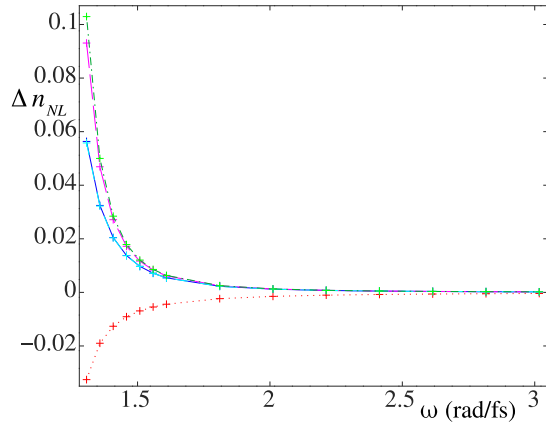
FIG. 5. The nonlinear shift of the refractive index Δn_{NL} vs the wave angular frequency ω, above the resonance and close to it, for an elliptic modulus $k = 0.15$. The color code is the same as in Fig. 1. The resonance frequency is $\lambda_r = 1.7$ μm.

evaluated from the numerical solution, which is a bit smaller than the input amplitude in this range of parameters. The angular frequency is not exactly constant, but varies as the frequency of the cnoidal wave solution (9) for fixed p and varying k. It is seen that although the NLS approximation is more accurate at small and moderate amplitudes, the cnoidal wave solution yields a more accurate value of the nonlinear shift of the index when the amplitude is very high, the threshold being located between the elliptic modulus $k = 0.5$ and 0.6, which would correspond to considerable intensities of about 100 and 160 TW/cm^2, for this set of parameters.

The situation is slightly different for values of the wave frequency that are higher than the resonance ($\omega > \Omega$). It is well known that the refractive index of the two-level model is less than 1 in this case, even in the linear case. Recall that c/n is the phase velocity; it is easily checked by direct computation that the corresponding group velocity is less than c. The same happens with the classical Lorentz theory, for which the frequency profile of the susceptibility is exactly the same.

Figure 5 presents an example of the computation of the nonlinear shift Δn_{NL} of the refractive index, above the resonance. Parameters have been chosen, however, in such a way that the index remains real whatever approximation is used, and the resonance effect clearly appears. In this domain, the Δn_{NL} computed according to the cnoidal wave solution has the wrong sign, while the NLS approximation gives a reasonable value. The approximation is quite accurate far away enough from resonance, where the nonlinear index remains moderate, but becomes much less accurate close to the resonance, as can be seen for a logarithmic plot of the error $n_{an} - n_{num}$, i.e., the difference between the index obtained numerically n_{num} and n_{an}, the one derived from an analytical formula, either the cnoidal wave solution or the NLS approximation, for the same data as in Fig. 5; see Fig. 6. The intensities range here between 7.5 TW/cm^2 and 46 TW/cm^2. The same evolution is found when the increase of nonlinearity is driven by the wave amplitude rather than by the proximity to resonance; see an example in Fig. 7.
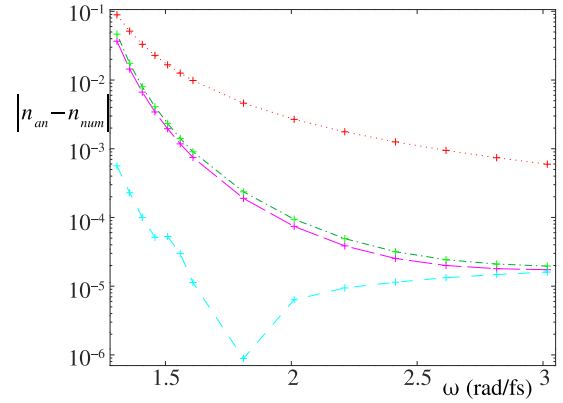

FIG. 6. The error $n_{an} - n_{num}$, for the same data as in Fig. 5, on a logarithmic scale.

B. Explanation and improvement for high intensities by means of *cn*

Figure 8 shows an example of profiles, in some special case with $\omega > \Omega$. As previously, we plot all components E, $\mathcal{W}$, d, and q of the numerical solution and compare them with the corresponding analytic expressions, as given by both the cnoidal wave solution and the NLS approximation. The intensity considered here is very large, about 13 TW/cm^2, which allows one to observe the development of modulation instability and the formation of a soliton train on a distance as short as the half length $L = 120$ μm of the computation box. It is seen that at this stage of soliton formation, the phase evolution computed from the constant amplitude solution of the NLS equation still reasonably agrees with that of the numerical solution.

We are mostly interested, however, in the domain where the wave amplitude can be considered as constant (up to $z = 80$ μm or a few more in Fig. 8). The agreement between the analytical and numerical profiles is rather satisfactory for all components except the population difference $\mathcal{W}$. $\mathcal{W}$ not only oscillates, but its mean values increase during the pulse,
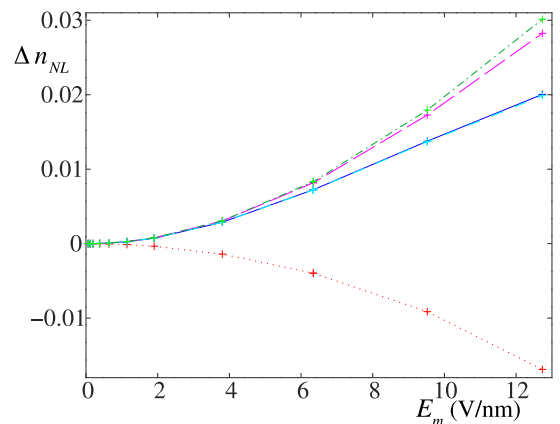

FIG. 7. The nonlinear shift of the refractive index Δn_{NL} vs the wave amplitude E_m. The color code is the same as in Fig. 1. The input assumes $p = 1.45$ rad fs^{-1}, with an elliptic modulus k varying from 0.001 to 0.2. The resonance wavelength is $\lambda_r = 1.7$ μm.
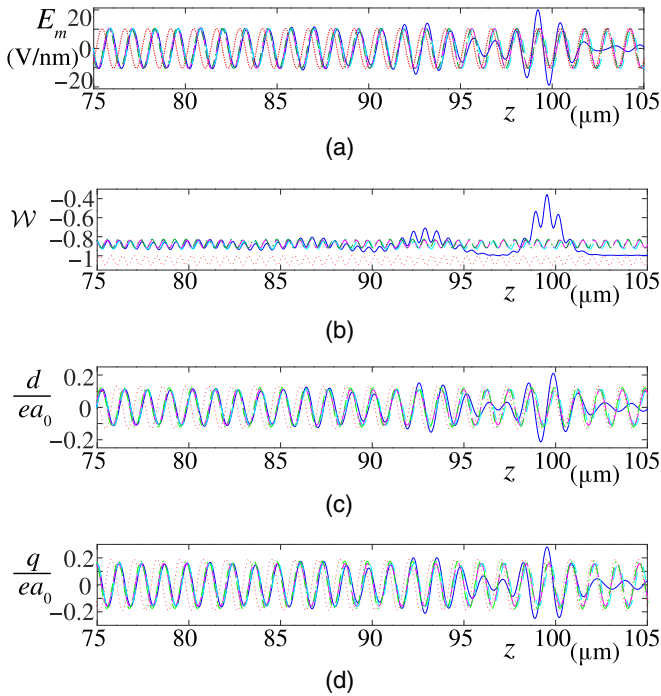
FIG. 8. The evolution of a square pulse, (a) electric field E, (b) population difference $\mathcal{W}$, (c) atomic dipole momentum d, (d) auxiliary field q. Only the part of the computation box representing the two-level medium is shown. The color code is the same as in Fig. 1. The resonance wavelength is $\lambda_r = 1.7\ \mu$m, the parameters of the initial data are $\omega_w = 1.6091\ \text{rad fs}^{-1}$, $k = 0.15$.

with respect to its value in the absence of light. The NLS approximation, however, provides this mean value $\mathcal{W}_0$ with a reasonable accuracy. The cnoidal wave solution, in contrast, does not; further, it yields unphysical values $\mathcal{W} < -1$. If we carefully consider its derivation, (see Ref. [13]), we see that the parameter $-l$ could be identified as the value of $\mathcal{W}$ in the absence of wave only for a localized wave, i.e., a soliton, since it is the exact traveling solution. Otherwise, it is only a constant shift above which $\mathcal{W}$ oscillates, as

$$\mathcal{W} = \frac{N}{\varepsilon_0 \hbar \chi \Omega} d^2 - l. \tag{33}$$

We see here that the identification of $-l$ as the value of the population difference $\mathcal{W}$ at thermodynamic equilibrium is valid for solitons only, while it remains an indeterminate constant for the cnoidal wave. This constant, however, can be evaluated by means of the NLS approximation, using expression (28) of $\mathcal{W}$, as

$$\mathcal{W}_0 = -l + \frac{l |\mu|^2 E_m^2}{\hbar^2} \left[\frac{(\Omega^2 + \omega^2)}{(\Omega^2 - \omega^2)^2} - \frac{1}{|\Omega^2 - \omega^2|} \right]. \tag{34}$$

Replacing l by $-\mathcal{W}_0$ in expressions (9)–(15) of the cnoidal wave solution yields a third analytic solution, which is shown by the pink dashed lines in all of the above figures. The values obtained by this improved cnoidal wave model are very close to the ones given by the NLS approximation. In other words, the cnoidal wave model is very accurate but does not provide

the mean value $\mathcal{W}_0$ of the population difference which is a key parameter, while NLS does allow one to compute it. However, the NLS approximation is a perturbation approach, and consequently its validity, in its very principle, is restricted to small or at least moderate values of the intensity, and its accuracy decreases as the wave amplitude increases. We obtain, however, estimations of the nonlinear shift of the index Δn_{NL} with still reasonable accuracy, even for quite large wave intensities, as show in the above examples.

For higher intensities, the cnoidal wave model is expected to remain valid; however, the analytic expression (34) of $\mathcal{W}_0$ does not. To find some nonperturbative analytic expression of it would obviously be an issue of interest, but we leave it for further investigation and use instead the value of $\mathcal{W}_0$ computed from the numerical solution. The corresponding corrected value of l can be reinserted in the expressions (9)–(15) of the cnoidal wave solution; the result is reported in all previous figures (light blue short dashes). The agreement is remarkable, showing that the main limitations to the accuracy of the cnoidal wave model (in the frame of the two-level atom model) are essentially due to $\mathcal{W}_0$.

In Figs. 2–7 above, the *cn* solution corrected with $\mathcal{W}_0$ given by the NLS approximation (pink long dashes) always remains very close to the NLS approximation itself (green dash-dotted line). This happens even when both appreciably depart from the numerical solution, which is almost perfectly fitted by the *cn* solution with the numerical $\mathcal{W}_0$. This implies that among all higher-order corrections to the NLS approximation, the one which involves $\mathcal{W}_0$ is far more important than the other, which could possibly be disregarded with respect to it.

The remaining inaccuracies come, on one hand, from the accuracy of the numerical resolution itself, which will remain finite whatever improvements can be implemented, and, on the other hand, from the dynamics of the population difference $\mathcal{W}$ itself. A transient regime arises as the pulse enters the medium, and it may show appreciable fluctuations of the oscillation amplitude of $\mathcal{W}$, as can be seen, for example, in Fig. 1. On the other side of the pulse, modulation instability leads to soliton formation. It is obviously accompanied by fluctuations of the amplitude of $\mathcal{W}$, which tends to be much larger than the fluctuations of the wave amplitude itself; see, e.g., Fig. 8.

V. CONCLUSION

We considered optical wave propagation within the frame of a two-level model and, using the perturbative expansion method, derived an asymptotic model of NLS type. The zero-harmonic or mean value term in the Fourier expansion of the population difference has been computed by this method; it appreciably modifies the nonlinear coefficient of the NLS equation and, consequently, the nonlinear shift of the refractive index. Especially for frequencies above the resonance, it changes the sign of this shift.

The NLS approximation not only yields the NLS equation itself, i.e., an asymptotic equation that describes the evolution of the field envelope, but also a complete approximate solution to the initial set of equations of the two-level model, which we have compared both with its numerical solution and with an exact analytical cnoidal wave solution.

It made prominent the importance of the evolution of the population difference for the accurate determination of the nonlinear index. However, disregarding this evolution may induce not only quantitative, but also qualitative error. Indeed, above the transition frequency, the nonlinear coefficient drawn from the susceptibility theory or from the rough NLS approximation, which does not take the population difference into account, has the wrong sign and would predict the stability of continuous waves, while modulation instability and soliton formation occur. Since, close to a resonance, the nonlinear coefficient is essentially due to it, the question of whether the nonlinear index changes its sign at a resonance is accessible in experiment.

It appeared that the cnoidal wave solution had to be corrected using an adequate value of the constant part of the population difference, which can be the expression of this quantity derived by means of the NLS approximation, if the amplitude is moderate, or the value obtained by the numerical solution, if the nonlinearity is so high that the perturbation scheme fails. Then the corrected cnoidal wave solution is in almost perfect agreement with the numerical solution, within the limits of our numerical accuracy.

The present study, however, is devoted to the continuous wave, or rather to pulses with long enough duration and constant enough amplitude so that they quite accurately match the continuous-wave model. We observed that the population difference may strongly fluctuate, at least when the pulse enters the medium and when it suffers modulation instability. Actual optical pulses, however, do not have a square profile, unless they are specifically prepared to match it. Profiles are usually bell shaped, with the most regular ones being frequently close to Gaussians or hyperbolic secants. Both this different shape and the actual pulse duration might influence the dynamics of the population difference, especially in the transient stage. One can imagine that this influence may have consequences on the dependency of the nonlinear shift of the index on the pulse duration and profile. Hence the study of the actual evolution of the population difference, including its fluctuations, would give further insight to the question.

The conclusions of this paper are, in principle, restricted to the purely theoretical lossless two-level model. In actual materials, many transitions are involved and absorption cannot be neglected. For conservative models, a study analogous to the present one can be performed. It should work in the same way on all of its aspects except the exact analytical solution, which may fail to exist for other models. An asymptotic model of the NLS type is expected in any situation. It is expected that the features observed here should occur for each of the population differences corresponding to any atomic transitions involved in the interaction between the light pulse and the actual material. Absorption can be incorporated into the analysis; in this case, the asymptotic model is expected to contain some absorption term in addition to the usual terms of the NLS equation. The absorption will occur for each atomic transition and modify the population differences. As it is well known, e.g., from the self-induced transparency, absorption is strongly dependent on the populations and modifies them. As a consequence, it cannot be expected that this further effect would cancel the one made prominent above; it should, rather, increase it.

APPENDIX: DERIVATION OF THE NLS APPROXIMATION FOR THE TWO-LEVEL MODEL

1. Assumptions and expansions

In this Appendix, we present the technical detail of the derivation of the asymptotic equation of the NLS type. It is more convenient to write the equations of the two-level model in the form (1)–(3), while Eqs. (4) and (5) are rewritten as

$$\frac{\partial^2 E}{\partial z^2} = \frac{1}{c^2} \frac{\partial^2}{\partial t^2}\left(E + \frac{N}{\varepsilon_0}d\right). \tag{A1}$$

Using the small parameter ε, we define slow variables as in (17) with no *a priori* assumption on the value of the velocity V. The electric field is expanded in both a Fourier series of the fundamental phase $\varphi = (\kappa z - \omega t)$ and in a power series of ε, as

$$E = \sum_{j=1}^{\infty} \sum_{p=-j}^{j} \varepsilon^j E_j^{(p)}(\tau, \zeta)e^{ip\varphi}. \tag{A2}$$

$\mathcal{W}$, q, and d are expanded in the same way, and the leading order of the electric field is fixed by (18).

In the same way, we assume that the expansions of d and q start with the terms $d_1^{(\pm 1)}$ and $q_1^{(\pm 1)}$, while $\mathcal{W}_0^{(0)} = -l$ represents the population difference at thermal equilibrium.

2. Resolution of the perturbation scheme

The expansions are then introduced in the set of equations, and the resulting system is solved order by order. First a nontrivial equation arises at order ε, and it is found that $\mathcal{W}_1^{(1)}$, $d_1^{(0)}$, and $q_1^{(0)}$ vanish, and that

$$q_1^{(1)} = \frac{i\omega}{\Omega}d_1^{(1)}, \quad d_1^{(1)} = \frac{2Y\Omega}{D}\mathcal{E}, \tag{A3}$$

where we have set for shortness

$$Y = \frac{l|\mu|^2}{\hbar}, \quad D = \Omega^2 - \omega^2, \tag{A4}$$

while the wave equation yields the dispersion relation, as $\kappa = n_0\omega/c$, with the linear refractive index n_0 defined as

$$n_0^2 = 1 + \frac{Q}{D}, \quad \text{with} \quad Q = \frac{2NY\Omega}{\varepsilon_0}, \tag{A5}$$

which can be made explicit to yield (19).

The first term in the expansion of the population difference, $\mathcal{W}_1^{(0)}$, is found at the following order ε^2 only; it is zero. At this order, it is also found that all second-harmonic terms $E_2^{(2)}$, $d_2^{(2)}$, and $q_2^{(2)}$ are zero, except

$$\mathcal{W}_2^{(2)} = \frac{2Y}{\hbar D}\mathcal{E}^2. \tag{A6}$$

The fundamental frequency terms satisfy $\mathcal{W}_2^{(1)} = 0$,

$$q_2^{(1)} = \frac{i\omega}{\Omega} d_2^{(1)} - \frac{2Y}{D} \frac{\partial \mathcal{E}}{\partial \tau}, \tag{A7}$$

$$d_2^{(1)} = \frac{2Y\Omega}{D} E_2^{(1)} + \frac{4iY\omega\Omega}{D^2} \frac{\partial \mathcal{E}}{\partial \tau}, \tag{A8}$$

while $E_2^{(1)}$ remains free, with the wave equation yielding the condition that V is the group velocity, $V = v_g = d\omega/d\kappa$.

Regarding the zero-harmonic components, it is found that $q_2^{(0)}$ vanishes and that $d_2^{(0)}$ is proportional to $E_2^{(0)}$, while no information about $E_2^{(0)}$ and $\mathcal{W}_2^{(0)}$ is obtained at this order.

At order ε^3, third-harmonic terms are obtained. First, we get

$$q_3^{(3)} = \frac{3i\omega}{\Omega} d_3^{(3)}, \quad d_3^{(3)} = \frac{2Y\Omega}{D_3} E_3^{(3)} - \frac{4Y^2\Omega}{l\hbar D_3 D} \mathcal{E}^3, \tag{A9}$$

where we set $D_3 = \Omega^2 - 9\omega^2$ for shortness. Using these expressions in the wave equation yields

$$E_3^{(3)} = \frac{-2QY}{l\hbar(n_0^2 - n_3^2)D_3 D} \mathcal{E}^3, \tag{A10}$$

where n_3 is the linear index for the third harmonic, defined by

$$n_3^2 = 1 + \frac{Q}{D_3}. \tag{A11}$$

In contrast, $\mathcal{W}_3^{(3)}$ is zero. These expressions are not needed to derive the NLS equation, but will be used to compare the present approximation with the numerical results.

The second-harmonic terms $E_3^{(2)}$, $d_3^{(2)}$, and $q_3^{(2)}$ are zero, while

$$\mathcal{W}_3^{(2)} = \frac{4Y}{\hbar D} \mathcal{E} E_2^{(1)} + \frac{4iY\omega}{\hbar D^2} \mathcal{E} \frac{\partial \mathcal{E}}{\partial \tau}. \tag{A12}$$

The fundamental harmonic components are

$$q_3^{(1)} = \frac{i\omega}{\Omega} d_3^{(1)} - \frac{2Y}{D} \frac{\partial E_2^{(1)}}{\partial \tau} - \frac{4iY\omega}{D^2} \frac{\partial^2 \mathcal{E}}{\partial \tau^2}, \tag{A13}$$

$$d_3^{(1)} = \frac{2Y\Omega}{D} E_3^{(1)} + \frac{4iY\omega\Omega}{D^2} \frac{\partial E_2^{(1)}}{\partial \tau} - \frac{2Y\Omega}{lD} \mathcal{W}_2^{(0)} \mathcal{E}$$
$$- \frac{4Y^2\Omega}{l\hbar D^2} \mathcal{E}|\mathcal{E}|^2 - \frac{2Y\Omega(\Omega^2 + 3\omega^2)}{D^3} \frac{\partial^2 \mathcal{E}}{\partial \tau^2}, \tag{A14}$$

while $\mathcal{W}_3^{(1)}$ is proportional to $\mathcal{E} E_2^{(0)}$. Using $d_3^{(1)}$ in the wave equation shows that $\mathcal{E}$ satisfies the differential equation (20), the coefficients of which are expressed as

$$\mathcal{B} = \frac{-\omega Q Y}{n_0 l\hbar c D^2}, \quad \mathcal{C} = \frac{-\omega Q}{2n_0 lcD}. \tag{A15}$$

3. Zero-order harmonic

The importance of this point has been emphasized in the body of the paper.

The equation that gives $\mathcal{W}_2^{(0)}$ is found at order ε^3. It reduces to

$$\frac{\partial \mathcal{W}_2^{(0)}}{\partial \tau} = \frac{4Y}{\hbar D^2}(\Omega^2 + \omega^2)\frac{\partial |\mathcal{E}|^2}{\partial \tau}. \tag{A16}$$

Here, $\mathcal{W}_2^{(0)}$ is obtained after integration, fixing the value of the integration constant by the assumption that if the pulse is localized, i.e., $\mathcal{E}$ vanishes at infinity, then $\mathcal{W}_2^{(0)}$ does also.

Making use of the obtained expression in Eq. (20) yields the NLS equation (23), in which

$$\Gamma = \frac{-QY\omega}{n_0 l\hbar c D^3}(3\Omega^2 + \omega^2), \tag{A17}$$

or, coming back to initial parameters, expression (24).

The zero-harmonic terms $d_3^{(0)}$ and $q_3^{(0)}$ are proportional to $E_3^{(0)}$ and $\partial E_2^{(0)}/\partial \tau$, respectively. However, the equations for $E_2^{(0)}$ and $E_3^{(0)}$ are only found at orders ε^4 and ε^5, respectively. It is seen that

$$\frac{\partial^2 E_j^{(0)}}{\partial \tau^2} = 0, \tag{A18}$$

for both $j = 2$ and 3, which, together with the assumption of a localized pulse, show that $E_2^{(0)} = E_3^{(0)} = 0$. Consequently, $d_2^{(0)}$, $\mathcal{W}_3^{(1)}$, $d_3^{(0)}$, and $q_3^{(0)}$ are also zero. We will not compute $\mathcal{W}_3^{(0)}$, which is not needed.

4. Solution of constant amplitude of NLS and Kerr effect

To investigate this hypothesis, the complete approximate solution is required. In the course of the derivation, both the second-harmonic and the rectified field terms of the population difference $\mathcal{W}$ have been computed. It can be expressed as

$$\mathcal{W} = \mathcal{W}_0^{(0)} + \varepsilon^2 \mathcal{W}_2^{(0)} + \varepsilon^2 \left(\mathcal{W}_2^{(2)} e^{2i\varphi} + cc+\right) + O(\varepsilon^3), \tag{A19}$$

in which the second-order terms in the expansion of $\mathcal{W}$ are given by formulas (A6) and (A16). Explicit computation yields the expression (28) of $\mathcal{W}$.

Pursuing the derivation a bit further, we can compute the harmonic terms that reduce to a third harmonic for d and q (we will neglect the third-harmonic term of E), so that

$$d = \varepsilon d_1^{(1)} e^{i\varphi} + \varepsilon^3 \left(d_3^{(1)} e^{i\varphi} + d_3^{(3)} e^{3i\varphi}\right) + cc + O(\varepsilon^4), \tag{A20}$$

and an analogous expression of q. Here, $d_1^{(1)}$, $d_3^{(1)}$, and $d_3^{(3)}$ are given by (A3), (A14), and (A9), respectively. The second involves the expression (A16) of $\mathcal{W}_2^{(0)}$, while $d_3^{(3)}$ involves $E_3^{(3)}$, which is given by (A10). For the stationary solution (25), the derivative terms are zero and we can impose that the higher-order arbitrary amplitudes $E_j^{(1)}$ ($j \geqslant 2$) also are zero.

We write, finally, the atomic dipole as expression (29), in which the coefficients a_1 and a_2 are expressed as

$$a_1 = \frac{-l|\mu|^4 \Omega(3\Omega^2 + \omega^2)}{\hbar^3(\Omega^2 - \omega^2)^3} \tag{A21}$$

and

$$a_3 = \frac{l|\mu|^4\Omega}{8\hbar^3\omega^2(\Omega^2-\omega^2)}. \tag{A22}$$

The third-harmonic resonance factor $D_3 = (\Omega^2 - 9\omega^2)$, which appears in the denominator of the expressions of $d_3^{(3)}$

involving $E_3^{(3)}$, and n_3 [Eqs. (A9)–(A11)], completely vanishes from the expression of a_3 due to algebraic simplification.

Using (A3), (A13), and (A9) in (30), and reducing the expression for the case of the stationary solution, we get the approximate solution for q given by (30).

[1] M. Sheik-Bahae, A. A. Said, T. H. Wei, D. Hagan, and E. W. Van Stryland, Sensitive measurement of optical nonlinearities using a single beam, IEEE J. Quantum Electron. **26**, 760 (1990).

[2] G. Boudebs and C. B. de Araújo, Characterization of light-induced modification of the nonlinear refractive index using a one-laser-shot nonlinear imaging technique, Appl. Phys. Lett. **85**, 3740 (2004)

[3] G. Boudebs, V. Besse, C. Cassagne, H. Leblond, and C. B. de Araújo, Nonlinear characterization of materials using the D4sigma method inside a Z-scan 4f-system, Opt. Lett. **38**, 2206 (2013).

[4] G. Boudebs, S. Cherukulappurath, H. Leblond, J. Troles, F. Smektala, and F. Sanchez, Experimental and theoretical study of higher-order nonlinearities in chalcogenide glasses, Opt. Commun. **219**, 427 (2003).

[5] D. G. Kong, Q. Chang, H. A. Ye, Y. C. Gao, Y. X. Wang, X. R. Zhang, K. Yang, W. Z. Wu, and Y. L. Song, The fifth-order nonlinearity of CS_2, J. Phys. B: At. Mol. Opt. Phys. **42**, 065401 (2009).

[6] V. Besse, G. Boudebs, and H. Leblond, Determination of the third and fifth-order optical nonlinearities: The general case, Appl. Phys. B **116**, 911 (2014).

[7] C. Wang, C. Fan, C. Yuan, G. Yang, X. Li, C. Ju, Y. Feng, and J. Xu, Third- and high-order nonlinear optical properties of an intramolecular charge-transfer compound, RSC Adv. **7**, 4825 (2017).

[8] T. Ning, X. Yu, L. Yin, and Q. Zhang, Third- and fifth-order optical nonlinearity in $PbO - BaO - Na_2O - Nb_2O_5 - SiO_2$ glass and glass-ceramic nanocomposite dielectrics, Optik **247**, 167943 (2021).

[9] J. A. Armstrong, N. Bloembergen, J. Ducuing, and P. S. Pershan, Interactions between light waves in a nonlinear dielectric, Phys. Rev. **127**, 1918 (1962).

[10] N. Bloembergen and Y. R. Shen, Quantum-theoretical comparison of nonlinear susceptibilities in parametric media, lasers and Raman lasers, Phys. Rev. **133**, A37 (1964).

[11] R. W. Boyd, *Nonlinear Optics* (Academic, San Diego, 1992).

[12] V. Besse, H. Leblond, and G. Boudebs, Fifth-order nonlinear susceptibility: Effect of the third-order resonances in a classical theory, Phys. Rev. A **92**, 013818 (2015).

[13] H. Leblond, Half-cycle soliton and periodic waves of arbitrarily high amplitude in a two-level system, Phys. Rev. A **99**, 053846 (2019).

[14] H. Leblond and C. Ciret, Cnoidal wave in a two-level medium: An alternative approach to nonlinear susceptibilities, J. Opt. **23**, 125502 (2021).

[15] T. Taniuti and N. Yajima, Perturbation method for a nonlinear wave modulation I, J. Math. Phys. **10**, 1369 (1969).

[16] H. Leblond, The reductive perturbation method and some of its applications, J. Phys. B: At. Mol. Opt. Phys. **41**, 043001 (2008).

[17] R. Y. Chiao, E. Garmire, and C. H. Townes, Self-Trapping of Optical Beams, Phys. Rev. Lett. **13**, 479 (1964).

[18] V. E. Zakharov and A. B. Shabat, Exact theory of two-dimensional self-focusing and one-dimensional self-modulation of waves in nonlinear media, JETP **34**, 62 (1972).

[19] C. R. Menyuk, R. Schiek, and L. Torner, Solitary waves due to $\chi^{(2)} : \chi^{(2)}$ cascading, J. Opt. Soc. Am. B **11**, 2434 (1994).

[20] W. E. Torruellas, Z. Wang, D. J. Hagan, E. W. Van Stryland, G. I. Stegeman, L. Torner, and C. R. Menyuk, Observation of Two-Dimensional Spatial Solitary Waves in a Quadratic Medium, Phys. Rev. Lett. **74**, 5036 (1995).

[21] A. Davey and K. Stewartson, On three-dimensional packets of surface waves, Proc. R. Soc. Lond. A **338**, 101 (1974).

[22] H. Leblond, Bidimensional optical solitons in a quadratic medium, J. Phys. A: Math. Gen. **31**, 5129 (1998).

[23] T. Colin, Rigorous derivation of the nonlinear Schrödinger equation and Davey-Stewartson systems from quadratic hyperbolic systems, Asymptot. Anal. **31**, 69 (2002).

[24] H. Leblond and D. Mihalache, Models of few optical cycle solitons beyond the slowly varying envelope approximation, Phys. Rep. **523**, 61 (2013).

[25] H. Leblond, Direct derivation of a macroscopic NLS equation from the quantum theory, J. Phys. A: Math. Gen. **34**, 3109 (2001).

[26] J. T. Stuart and R. C. DiPrima, The Eckhaus and Benjamin-Feir resonance mechanisms, Proc. R. Soc. London A **362**, 27 (1978).

[27] K. Tai, A. Hasegawa, and A. Tomita, Observation of Modulational Instability in Optical Fibers, Phys. Rev. Lett. **56**, 135 (1986).